Insight in ultrasonic shear reflection parameters by studying temperature and limonene influence on cocoa butter crystallization

Annelien Rigolle[a,c], Imogen Foubert[a,c], Jan Hettler[b], Erik Verboven[b], Arvid Martens[b], Ruth Demuynck[a,c], and Koen Van Den Abeele[b]

[a]KU Leuven Kulak, Research Unit Food & Lipids, Department of Molecular and Microbial Systems Kulak, Etienne Sabbelaan 53, 8500 Kortrijk, Belgium

[b]KU Leuven Kulak, Research Unit Wave Propagation and Signal Processing, Department of Physics Kulak, Etienne Sabbelaan 53, 8500 Kortrijk, Belgium

[c]Leuven Food Science and Nutrition Research Centre (LFoRCe), KU Leuven, Kasteelpark Arenberg 20, 3001 Heverlee, Belgium

Corresponding author: Annelien Rigolle
Phone: +32 (0) 56 24 62 57
Fax: +32 (0) 56 24 69 99
E-mail: Annelien.Rigolle@kuleuven-kulak.be

Keywords : cocoa butter, crystallization, ultrasound, shear reflection, in-line monitoring

In this study an inverse model was developed to derive relevant ultrasonic parameters from ultrasonic shear reflectometry measurements. The inverse model includes four variable parameters: t_{ind} (induction time), K (crystallization rate), v_{s2} (shear ultrasonic velocity) and a_{s2} (shear ultrasonic attenuation coefficient). Both the temperature effect and the effect of a minor component limonene (in different concentrations) on the isothermal crystallization of cocoa butter were studied with the ultrasonic shear reflectometry technique and associated inverse model. Subsequently, the ultrasonic parameters were compared with results of conventional techniques to monitor fat crystallization (DSC, PLM). The study shows that t_{ind} and K provide information on the kinetics of the microstructure development. The parameter v_{s2} is related with the equilibrium SFC, while a_{s2} is both influenced by the SFC and the organization of the crystals in the network, yielding information about the microstructure of the crystallized samples.

Industrial relevance: The microstructure of crystallized fat determines to a large extent the macroscopic properties of fat rich products, such as texture, mouthfeel,… Hence, monitoring the crystallization behavior (including not only the primary crystallization but also the microstructural development) during the production process is of utmost importance in order to obtain high quality end products. The ultrasonic shear reflectometry technique is a fast non-destructive technique which provides quantitative data about the crystallization process based on an inverse model. The simplicity of the technique offers potential for inline control. This

may be beneficial to evaluate the crystallization process under different process conditions and to stimulate product innovation as more insight can be obtained in the microstructure development of new products.

1. Introduction

As the fat crystallization process determines to a large extent the quality of fat containing food products, several methodologies have been proposed to monitor the fat crystallization process. These techniques differ in the fat crystallization features they measure, and monitor various aspects of the fat crystallization process on multiple length scales.

Different structural levels can be distinguished in a fat crystal network. The crystallization process starts with the primary crystallization whereby the triacylglycerols (TAG) form crystalline lamellae. As the fatty acid chains of the TAG can adopt different molecular arrangements, distinct packing modes arise which result in different polymorphic forms with specific physical properties. The crystalline lamellae stack in crystalline nanoplatelets with dimensions in the hundred-nanometres range (Marangoni et al., 2012). The nanoplatelets then aggregate further through van der Waals attraction and clot to form larger clusters which interact even further, finally resulting in the formation of a continuous three-dimensional fat crystal network. The number, size, shape and spatial distribution of the particles and clusters of sizes between 1 and 200 μm define the microstructure, which is known to have an enormous influence on the macroscopic properties of fat products (Acevedo et al., 2011; Narine and Marangoni, 1999).

The nanoscale structures can be investigated by X-ray diffraction (XRD): the different polymorphic forms have characteristic wide angle XRD patterns, while small angle XRD patterns can be used to determine the thickness of the individual crystalline lamella and even the crystalline domains (which correspond to the thickness of the nanoplatelets) via Scherrer analysis (Acevedo et al., 2011). As an alternative, various types of microscopy can be applied to visualize the different structure levels. Cryogenic transmission electron microscopy has been used to expose the nanoscale structures, whereas polarized light microscopy (PLM) is often used to display the microstructural level (Acevedo et al., 2011; Marangoni et al., 2012). Although very valuable information can be obtained with microscopy, the technique also has some drawbacks. The sample material between the glass slides must be sufficiently thin in order to limit the attenuation of the transmitted light. This leads to growth restricted to one dimension

(Ghotra et al., 2002). In addition, quantitative data cannot be directly obtained from microscopy pictures.

Besides the structural rearrangements during crystallization, other properties of this liquid to solid transition can be probed. For instance, the relative amount of solid substance, better known as the solid fat content (SFC), can be determined by pulsed nuclear magnetic resonance (pNMR). As crystallization is an exothermic reaction, the released heat can also be used as a measure for the amount of crystallized material. This principle is applied when using differential scanning calorimetry (DSC) to monitor fat crystallization (Foubert et al., 2003). Finally, the crystallization process can also be followed by changes in the viscoelastic properties revealing the fluid and/or solid character of the sample system. This can be done using oscillatory rheology (De Graef et al., 2006) or using a viscometer (Dhonsi and Stapley, 2006).

The different techniques discussed above are the conventional techniques used to monitor fat crystallization processes, each with their advantages and disadvantages, but with the common limitation that they cannot be used for inline monitoring and control. Inline methods to monitor fat crystallization could have significant economic benefits, and therefore, there is a constant search for alternative, non-destructive techniques that can be used for inline inspection. Furthermore, the crystallization depends on the process conditions (temperature, shear, time) applied (Afoakwa et al., 2008) and it is therefore critical to monitor the crystallization process under the same process conditions, what is done automatically with an inline technique. NMR-MOUSE (Nuclear Magnetic Resonance - mobile universal surface explorer), Laser backscattering, Near-Infrared (NIR) spectroscopy and ultrasonic techniques have been suggested. NMR-MOUSE can be utilized for inline SFC measurements, but the technique is limited to static conditions and is less accurate than ultrasonics (Martini et al., 2005a). NIR spectroscopy allows to obtain microstructural information related to the size, shape and quantity of crystals via correlations between NIR spectra and measurements of viscosity and crystal content. Although these correlations are derived statistically and the relationship with the crystallization process is unclear (Bolliger et al., 1999), Svenstrup et al. (2008) demonstrated that NIR spectroscopy could distinguish between different tempering procedures. Furthermore, NIR spectroscopy has also been applied for the on-line determination of the fat content of meat (Wu & Sun, 2013). Laser backscattering can be applied to monitor changes in particle size distribution during crystallization, and although the total particle count correlates well with the amount of crystallized fat, it does not measure the solid fat content in a direct way and merely serves as an estimation (Hishamuddin et al., 2011).

Ultrasonic inspection is the most frequently studied non-destructive technique, because it is highly suitable for inline monitoring: capable of rapid and precise measurements, relatively inexpensive, non-hazardous, fully automatable and usable under stirring conditions (McClements & Povey, 1992; Martini et al., 2005b; Garbolino et al., 2000). For clarity, low intensity ultrasound is used which does not have any effect on the food product, in contrast to the high power ultrasound which is used to alter food properties or facilitate production processes (Patist & Bates, 2008). A selection of measurement set-ups for ultrasonic crystallization monitoring have been described by Rigolle et al. (2015). Commonly, most research studies deal with longitudinal or pressure waves whereby particles move in the same direction as the propagated wave. The (reflection and) transmission of pressure waves can be used to determine the SFC as this property is correlated with the ultrasonic velocity. A disadvantage of this methodology is that it is limited to low SFC levels or thin materials due to the high attenuation of crystallized fat (Singh et al., 2004). Nonetheless, data on attenuation can provide additional information about the polymorph (Häupler et al., 2014) or microstructure (Martini et al. 2005c).

In Rigolle et al. (2015), we developed an ultrasonic shear reflection technique to monitor fat crystallization. The main advantage of applying a reflection technique is that no problems with excessive attenuation of the fat arise. Furthermore, shear or transverse waves, where the movement of the particles is perpendicular to the direction of the propagating wave (McClements, 1997), seem more sensitive to changes in microstructure than pressure waves, as the former require a medium that displays shear elasticity (Létang et al., 2001) to be propagated. In Rigolle et al. (2015) the shear reflectometry technique has been introduced together with an interpretation of the experimental results. In the present article, an inverse model is developed to derive quantitative parameters from the experimental results. Subsequently, these ultrasonically obtained parameters are compared with data from conventional techniques, such as DSC and PLM, to shed light on the interpretation of these parameters. To obtain relevant data for model validation, the crystallization process was modified in two ways: by changing the crystallization temperature and by adding a minor component limonene. Limonene is a diterpene, which is naturally present in the D-form in ethereal oils of lemon and orange and is relevant in a reduced fat chocolate context (Beckett, 2001; Do et al., 2008). The fat content affects the rheological and textural properties of chocolate (Afoakwa et al., 2008) and cannot be reduced without any effect on quality. Therefore, a viscosity adjusting component should be added to reduced-fat chocolate and a US Patent by Beckett (2001) states that adding limonene

(in a concentration of up to 5% by weight) to a reduced-fat chocolate results in a lower viscosity and a softer chocolate, that melts more easily in the mouth, compared with the original reduced-fat chocolate without limonene. However, limonene drastically modifies the crystallization process by lowering the SFC, accelerating polymorphic transitions and changing the microstructure development (Do et al., 2008; Miyasaki et al., 2015; Ray et al., 2011).

2. Materials and Methods

2.1 Materials

The used cocoa butter was a standard factory product of West-African origin kindly provided by Barry Callebaut (Wieze, Belgium). D-Limonene (97%) was purchased from Sigma-Aldrich and was added to the melted cocoa butter at 85°C in concentrations of 1%; 2.5%; 5% and 7.5% by weight. The samples were then stirred for 10 minutes with a magnetic stir plate to obtain a homogeneous mixture.

2.2 Ultrasonic shear reflectometry measurements

2.2.1 Experiments

The experimental set-up for the shear reflectometry measurements is extensively described in Rigolle et al. (2015). In brief, a shear wave transducer (V154-RB, 12.7 mm active diameter, 2.25 MHz central frequency, Olympus Corporation, Tokyo, Japan) is attached to the bottom side of a plexiglass plate, above which an aluminum sample holder (60 mm diameter) is placed. Liquid cocoa butter (20g) at 30°C, with or without limonene, is poured into the sample holder to form a layer of 7.7 to 8 mm. The sample holder is surrounded by a container filled with water, which is kept at constant temperature by refreshing it, using a pumping system (Masterflex L/S, Metrohm, Belgium), with water from a cryostat (RC6 LAUDA, Lauda-Königshofen, Germany) at a fixed temperature. The experiments were carried out in a temperature controlled room, and the temperature of the water bath and of the fat sample was logged by two 80TK thermocouple modules (N.V. Fluke Belgium S.A, Gent, Belgium). A PXI-5412 arbitrary waveform generator card (National Instruments, Austin, Texas, USA) was used to produce electric signals which were converted into ultrasonic shear waves by the shear wave transducer. Excitations were typically performed at 1 MHz. A PXI-5122 data acquisition card (National Instruments, Austin, Texas, USA) was used to register the electric signals which were converted from the reflected ultrasonic shear waves by the same transducer. The signals were averaged over 128 realizations. The determination of the shear wave reflection coefficient (swRC) is based on a relative measurement with an empty sample holder as reference. Every 10 s, the reflected signal from the plexiglass-sample column above the shear wave transducer was monitored and processed to obtain the evolution of the shear wave reflection coefficient during crystallization by

calculating the ratio of the maximum amplitude of the frequency spectrum of the current signal to the reference signal, as expressed in Equation 1.

$$\mathrm{swRC} = \frac{\max(\mathrm{FFT}(\text{sample signal}))}{\max(\mathrm{FFT}(\text{reference signal}))} \quad (1)$$

All measurements were carried out at least in triplicate.

2.2.2 Parameter inversion

A multi-parameter model (see Theory section for details) was fitted to the data series by applying a non-linear regression using Matlab®. The sum of squared residuals between the observed and predicted values of the swRC was minimized by a Levenberg-Marquardt algorithm. Based on physical considerations and some assumptions, a large number of parameters could be considered fixed (see section 3.3). The final fitting was therefore performed using only 4 free parameters. Initial guess values for these parameters were automatically calculated from overall characteristics of the experimental data (periodicity, asymptote, oscillation amplitude, etc).

2.3 DSC measurements

A DSC Q2000 with a Refrigerated Cooling System 90 (TA Instruments, New Castle, Del., U.S.A.) and nitrogen as purge gas was used to perform the isothermal DSC experiments. The baseline was calibrated with sapphire (TA Instruments, New Castle, Del., U.S.A.) and indium (TA Instruments, New Castle, Del., U.S.A.). The samples (6 mg to 15 mg) were sealed in Tzero hermetic aluminum pans (TA Instruments, New Castle, Del., U.S.A.) and an empty pan was used as a reference.

The following time-temperature program has been applied: holding at 65°C for 15 minutes to erase all crystal memory, cooling at 10°C/min to the isothermal crystallization temperature (18°C or 20°C) and holding at that temperature until crystallization is finished. Next, the sample was melted at 5°C/min to obtain the melting profile of the crystallized sample. Universal Analysis 2000 software version 4.5 A (TA Instruments, New Castle, Del., U.S.A.) was used to determine the peak onset and peak maximum in the crystallization curves and the area of the melting peak, which was integrated with a linear baseline. All experiments were performed at least in triplicate.

2.4 Polarized light microscopy measurements

The microstructure development during crystallization was studied by means of a polarized light microscope Olympus BX51 (Olympus Optical Co. Ltd., Tokyo, Japan) equipped with a

digital camera Infinity 2 (Lumenera corporation, Ontario, Canada). One drop of the liquefied sample (pure cocoa butter or cocoa butter with 2.5% and 7.5% limonene at 85°C) was transferred to a preheated (85°C) carrier glass with a hot (85°C) glass Pasteur pipette, and a preheated (85°C) covering slide was put on the sample. Subsequently, the sample was placed on a temperature-controlled Linkam PE120 stage (Linkam Scientific Instruments, Surrey, UK). The following time-temperature combination has been applied: heating to 65°C and holding for 15 minutes to eliminate all crystal nuclei, followed by cooling at 10°C/min to the isothermal crystallization temperature (18°C or 20°C) and holding at that temperature until crystallization is finished. At different times after crystallization started, the formed crystals were photographed using the Infinity capture software provided by Lumenera using a 200x magnification.

2.5 Statistics

The ultrasonic and DSC parameters were analyzed by analysis of variance (ANOVA) using RStudio software. Tukey Honest Significant Differences was used as post hoc test and differences are considered significant at $p<0.05$.

3 Theory

3.1 Typical evolution of the swRC during crystallization

The propagation of shear waves in crystallizing cocoa butter has been extensively discussed in Rigolle et al. (2015) and the reader is kindly referred to this paper for more detailed information. Figure 1 clarifies the relation between the oscillatory behavior of the swRC during crystallization (Fig. 1A) and the propagation of shear waves in the sample (Fig. 1B). At the start of the monitoring, the sample is in a fully liquid state (Phase 1). Since the weak molecular bonds of liquids do not support shear waves, total reflection occurs and the swRC approximates 1. When a crystallized layer of cocoa butter is formed on top of the plexiglass plate, the emitted pulse partially reflects from the plexiglass-sample boundary and partially travels across the crystallized layer until it reaches the boundary between crystallized and liquid cocoa butter (Phase 2). At this boundary, the transmitted pulse is totally reflected and it will interfere with the direct reflected pulse generated at the boundary between plexiglass and crystallized cocoa butter. The oscillatory behavior of the swRC during Phase 2 can then be explained by an alteration of constructive and destructive interferences of the two reflected pulses. Furthermore, during this period, the amplitude of the swRC oscillation is decreasing in time, which can be explained by the accrued attenuation of the pulse travelling across the crystallized sample.

When the thickness of the crystallized layer increases, the accumulated damping effect will also increase, resulting in a lower amplitude of the second reflected pulse, and consequently in a less pronounced interference effect. Ultimately, at a certain crystallized layer thickness, the accrued attenuation fully extinguishes the second reflection (Phase 3), and no interference effect occurs anymore, resulting in a stagnation of the swRC.

3.2 Modeling the evolution of the swRC

The swRC behavior during Phase 2 can be mathematically described by Equation 2 (Rigolle et al., 2015) whereby Table 1 lists the various model parameters. Where appropriate, the subscripts 1 and 2 refer to the value of the parameter belonging to medium 1 (plexiglass) and medium 2 (crystallized cocoa butter) respectively. The analytical model for swRC can be used to fit the experimental results in order to deduce quantitative parameters from the experimental curves describing the crystallization process. In order to do so, the time dependence of the thickness of the crystallized layer ($d(t)$) should be estimated by a function that closely follows the characteristics of a isothermal crystallization process. As in Rigolle et al. (2015), the Foubert model (Equation 3) (Foubert et al., 2002), written as the fraction of crystallizable fat at time t, is used to define a normalized sigmoidal function (Equation 4) describing the fraction of crystallized fat. Equation 4 was then transposed to simulate the time evolution of the crystallized layer thickness as expressed in Equation 5, where the parameter d^* is related to the thickness of the crystallized layer whereby complete attenuation of the secondary pulse arises.

$$\mathrm{swRC}(t)=\frac{\left[\rho_2 v_{s_2}\left(1-ia_{s_2}\right)-\rho_1 v_{s_1}\right]-\left[\rho_2 v_{s_2}\left(1-ia_{s_2}\right)+\rho_1 v_{s_1}\right]\exp\left(2i\frac{\omega}{v_{s_2}}d(t)\right)\exp\left(-2\frac{\omega}{v_{s_2}}a_{s_2}d(t)\right)}{\left[\rho_2 v_{s_2}\left(1-ia_{s_2}\right)+\rho_1 v_{s_1}\right]-\left[\rho_2 v_{s_2}\left(1-ia_{s_2}\right)-\rho_1 v_{s_1}\right]\exp\left(2i\frac{\omega}{v_{s_2}}d(t)\right)\exp\left(-2\frac{\omega}{v_{s_2}}a_{s_2}d(t)\right)} \quad (2)$$

$$y(t)=y\left(t;n,y_0,K\right)=\left[1+\left(y_0^{\,1-n}-1\right)e^{-(1-n)Kt}\right]^{\frac{1}{1-n}} \quad (3)$$

$$S(t)=S\left(t;n,y_0,K\right)=\frac{1}{y_0}\left(y_0-y(t)\right) \quad (4)$$

$$d\left(t\right)=d\left(t;n,y_0,K\right)=d^{*}.S\left(t;n,y_0,K\right) \quad (5)$$

$$\mathrm{swRC}_{\infty}=\lim_{t\to\infty}\mathrm{swRC}(t)=\frac{\rho_2 v_{s_2}(1-ia_{s_2})-\rho_1 v_{s_1}}{\rho_2 v_{s_2}(1-ia_{s_2})+\rho_1 v_{s_1}} \quad (6)$$

$$t_{ind}=\frac{-\ln\left(\frac{\left(1-x/100\right)^{1-n}-1}{y_0^{\,1-n}-1}\right)}{(1-n)K} \quad (7)$$

Table 1: List of model parameters, with reference to Equations (2-7)

ρ	Density (kg/m³)
v_s	Shear ultrasonic velocity (m/s)
a_s	Shear ultrasonic attenuation coefficient (-)
$d(t)$	Thickness of the crystallized layer of medium 2 at time t (m)
ω	Angular frequency (rad/s)
$y(t)$	Fraction of crystallizable fat at time t (-)
y_0	Initial fraction of crystallizable fat (-)
K	Crystallization rate (1/min)
n	Asymmetry characteristic of the crystallization curve (-)
$S(t)$	Normalized fraction of crystallized fat at time t (-)
d^*	Parameter related to the thickness of the crystallized layer whereby complete attenuation of the secondary pulse arises (m)
t_{ind}	Induction time (min)

Note that Equation 2, which is time dependent as the thickness of the crystallized layer gradually increases, simplifies to a constant value given by Equation 6 in Phase 3 ('long time' asymptote) due to the factor $\exp\left(-2\,d(t)\,\omega\,a_{s_2}/v_{s_2}\right)$ in the numerator and denominator which approximates zero at a critical value of the product of d and a_{s2}.

3.3 Inverse model

The model described in section 3.2 has a large number of variable parameters. Based on physical considerations and some assumptions, a number of parameters can be considered fixed, in order to keep the model simple and facilitate the inverse modeling.

First of all, the material parameters of plexiglass are fixed, whereby ρ_1 is set to 1180 kg/m³, v_{s1} to 1200 m/s and a_{s1} to zero as the attenuation of plexiglass is assumed to be negligible. The density of crystallized cocoa butter (ρ_2) is set to 920 kg/m³ based on Maleky and Marangoni (2011). The shear ultrasonic velocity (v_{s2}) and shear ultrasonic attenuation (a_{s2}) are parameters that can provide interesting information about the crystallized sample, and consequently they are considered as being variable parameters. They are however assumed to be constant over time and over the entire crystallized layer.

The evolution of the crystallized layer over time, $d(t)$, is governed by Equations 3-5 which in turn comprise four parameters: y_0, K, n, which are parameters of the Foubert model, and d^*. The physical interpretation of the parameter y_0, the initial fraction of crystallizable fat, is not straightforward. A sensitivity analysis, displayed in Figure 2, varying the parameter y_0, while all other parameters remain constant, showed that this parameter induces a horizontal shift of the results, implying that y_0 is related to the induction time (t_{ind}). The relationship between y_0 and t_{ind} can be mathematically expressed as in Equation 7, derived by Foubert et al. (2002), who defined t_{ind} as the time needed to reach x% of crystallization. Because shear waves need a sample with a certain amount of crystallized material before they can be propagated, we set x to 5 instead of 1 as was done for the DSC curves in Foubert et al. (2002). During the current research work, and supported by results obtained in previous studies (e.g. Calliauw et al., 2008; Rigolle et al., 2015b), the crystallization rate parameter K was found to be strongly correlated with n, describing the asymmetry of the crystallization curve (Foubert et al., 2002). The influence of the parameter K, representing the crystallization rate, has already been investigated in Rigolle et al. (2015), and it was found that K is associated with the periodicity of the oscillations. More specifically, a higher value of K gives rise to faster oscillations. Therefore, it was decided to consider K variable and fix n to a constant value of 8 based on preliminary results. The same problem of high correlation with parameter K arose for the thickness parameter d^*. Again, it was opted to fix d^* to the average value of all preliminary inversion results, being 0.002 m, in order to make the estimation of the other parameters more reliable.

The above results in a model with 4 remaining parameters: t_{ind} (induction time), K (crystallization rate), v_{s2} (shear ultrasonic velocity) and a_{s2} (shear ultrasonic attenuation coefficient). Despite the

assumptions of fixed n and d^*, the fit was still very good with R^2 values that were never below 0.8, and in most cases above 0.9. This means that there is an acceptable fit with only four parameters whose values can be properly interpreted. Figure 3 illustrates the fitting of the described model to experimental data demonstrating that the 4-parameter model is able to fit the experimental curves in a sufficient manner.

The initial values for the kinetic parameters (y_0 and K) are estimated by the positions of the maxima and minima of the oscillations. Because of the factor $\exp\left(-2\,d(t)\,\omega\,a_{s_2}/v_{s_2}\right)$, the overall damping of the oscillations is controlled by a_{s2}. In addition, the parameter v_{s2} appears to be the main parameter controlling Equation 6, defining the asymptotic value of the swRC (i.e. in the case of no interferences). Consequently, initial values of a_{s2} and v_{s2}, required as input for the nonlinear inversion routine, can be obtained by determining the characteristic oscillation dampening and the value of the final swRC from the experimental data respectively. In all inversions, an initial value of 0.15 for a_{s2}, derived on the basis of preliminary experiments, appeared to be appropriate to avoid that the iterative process gets stuck in a local minimum.

4 Results and Discussion

4.1 Effect of temperature

To gain more insight into the four free parameters of the inverse model first the influence of the crystallization temperature on the ultrasonic parameters was explored. A lower crystallization temperature corresponds to a higher supercooling and therefore a higher driving force for crystallization, which significantly modifies the crystallization behavior, both kinetically and thermodynamically.

4.1.1 Ultrasonic measurements

Figure 4 illustrates the differences in the evolution of the swRC during crystallization of pure cocoa butter at 18°C and 20°C with one exemplary curve of each temperature and Table 2 shows the inversion results for both temperatures. It can clearly be observed that the oscillations start earlier and are damped faster at 18°C compared to 20°C. The lower crystallization temperature of 18°C led to a significantly shorter t_{ind} and higher K, both suggesting a faster crystallization process. Furthermore, a significantly higher v_{s2} (in agreement with a lower asymptotic value of swRC) was observed for the lowest crystallization temperature. A higher v_{s2} indicates a more elastic sample, as it corresponds to a lower end swRC, meaning that a

greater part of the signal is transmitted into the sample because it is more acoustically similar to plexiglass. The parameter a_{s2} did not differ significantly between both temperatures, although it was slightly lower at 20°C than at 18°C.

4.1.2 Conventional techniques

DSC isothermal crystallization curves of pure cocoa butter at 18°C and 20°C (detailed results not shown) exhibited two exothermic events, corresponding to a two-step crystallization process with an initial α crystallization and a consecutive polymorphic transition to β' as described by several authors who have monitored the isothermal crystallization of cocoa butter at similar temperatures (Dewettinck *et al*., 2004; van Malssen, *et al*., 1999). As the α peak overlapped with the cooling and equilibration phase to the isothermal temperature, it was not very noticeable. The peak onset (t_{onset}) and peak maximum (t_{peak}) of the main crystallization peak, representing the α mediated β' crystallization, are presented in Table 3 and it can be concluded that the crystallization process was faster at 18°C compared to 20°C. Furthermore, the total melting enthalpy (ΔH_{tot}), as a measure for the equilibrium SFC, was significantly higher at 18°C compared to 20°C (Table 3), which corresponds to literature (Talbot, 2009).

DSC measures the heat flow and therefore the primary crystallization process consisting of nucleation and crystal growth, but is not sensitive to the aggregation of these crystals as this process does not release heat. Therefore, PLM images were taken at certain moments in time during the crystallization process. The birefringent character of fat crystals makes the crystals appear bright between two crossed polarized filters, while the liquid oil remains dark (Acevedo et al., 2011). The pictures (detailed results not shown) confirmed that the crystals are more rapidly formed at a temperature of 18°C compared to 20°C, and also more crystals were formed at 18°C, but no clear effects on the shape and size of the crystals could be detected.

4.1.3 Comparison of ultrasonic and conventional techniques

Before attempting to link the ultrasonic shear reflectivity results to DSC and PLM, we must remark that the results of diverse techniques can only be relatively compared since different measuring techniques monitor distinct features of the crystallization process and equipment design differs greatly, leading to different heat transfer rates and sample sizes which can influence the crystallization process.

Since t_{ind} obtained by the ultrasonic technique was much longer than the first small peak observed by DSC during and just after the cooling phase, it can be concluded (even taken into

account the difference in sample size) that the initial small α crystallization peak cannot be detected by the swRC measurements. This can be understood by reminding that shear waves need a material with a developing or established shear elasticity, such as a crystal network, to be propagated and during the α crystallization there was an insufficient amount of crystals to form such a network. On the other hand, the shorter t_{ind} measured by the ultrasonic technique at 18°C compared to 20°C (Table 2) is in accordance with the earlier t_{onset} of the β' peak observed with DSC (Table 3) and the more rapid formation of crystals visualized with PLM (detailed results not shown).

The higher *K* parameter at 18°C in the ultrasonic experiments, is more difficult to link to the conventional techniques as no real growth rate could be calculated from the DSC results because the two crystallization peaks were not completely separated making it impossible to fit a crystallization model to the second peak. As the time lag between peak onset and peak maximum of the β' peak was similar for both temperatures (Table 3), we could assume that there was no dramatic difference in the growth rate of the β' polymorph, while a significant difference was observed for *K* deduced from the ultrasonic experiments (Table 2). This suggests that the ultrasonic *K* does not monitor the primary crystallization itself.

The parameter v_{s2} was significantly higher at the lowest crystallization temperature (Table 2) suggesting a more elastically rigid material at that processing temperature, which could be partially explained by the higher SFC, as observed by the higher ΔH_{tot} (Table 3). However, the mechanical properties, including the elasticity, are not only determined by the SFC, but also by the structure of the fat crystal network (Brunello et al., 2003). The slightly higher a_{s2} at 18°C, although not significant (Table 2), can also be seen in this context as a higher amount of crystallized material damps out the ultrasonic signal to a greater extent. Yet, again, also the attenuation coefficient not only depends on the SFC, but also on the microstructure and especially on the crystal size (Martini et al., 2005). However, since, visually, only slight differences in the microstructure could be detected (detailed results not shown) no hard conclusions can be drawn about the influence of microstructure on the ultrasonic parameters.

In the next section, it will be shown that the microstructure was more drastically altered by the addition of limonene in accordance to what has been reported by Ray et al. (2011) and these results will thus allow to better investigate the influence of microstructure on the ultrasonic parameters.

4.2 Effect of limonene

In order to investigate the influence of the microstructure on the parameters of the ultrasonic shear reflection technique, we considered the isothermal crystallization at 18°C of pure cocoa butter and samples blended with four different concentrations of limonene (1%; 2.5%; 5% and 7.5%). We analyzed the ultrasonic parameters using the inverse model and at the same time, the crystallization behavior of these blends was studied by conventional techniques (DSC and PLM). The results of the various techniques were compared to infer the significance of the parameters of the inverse model.

4.2.1 Ultrasonic measurements

One exemplary curve of the evolution of the swRC during crystallization of pure cocoa butter and cocoa butter samples with addition of 2.5% and 7.5% limonene is depicted in Figure 5. Table 4 presents the list of parameters of the ultrasonic shear reflection technique obtained by the inverse model for pure cocoa butter and for cocoa butter with the addition of different concentrations of limonene, isothermally crystallized at 18°C. It can be observed that both the start and the periodicity of the oscillations as well as the end swRC were influenced by the addition of limonene. The presence of limonene had no significant impact on t_{ind} (considering the error bars), although there was an increasing trend from 0% to 5% limonene. An increasing trend as function of the concentration of limonene was also visible for the *K*-parameter, while only the highest limonene concentration was significantly different from the pure cocoa butter. The higher *K* with addition of limonene corresponds to the more rapid succession of oscillations in the presence of limonene, whereby also a concentration effect was visible. Interestingly, v_{s2} revealed significant differences between the highest concentrations limonene (5% and 7.5%) and pure cocoa butter. Moreover, a general decreasing trend was observed with increasing limonene concentrations for this parameter, which is associated with the increasing end swRC with increasing limonene concentrations, noticeable in Figure 5. On the other hand, no significant differences could be detected in the a_{s2}-parameter and hence the attenuation was similar for all samples.

4.2.2 Conventional techniques

Concurrently with the ultrasonic shear wave reflectivity study, isothermal DSC crystallization experiments were performed at 18°C to gain insight into the kinetics of the primary crystallization. The parameters t_{onset} and t_{peak} of the main crystallization peak are summarized in Table 5. A striking feature of these results is that the behavior for the highest limonene concentration, which exhibited a significantly slower crystallization (higher t_{onset} and t_{peak}) than

the pure cocoa butter, did not follow the trend of the other limonene concentrations, exhibiting a faster crystallization (lower t_{onset} and t_{peak}) compared with pure cocoa butter. On the other hand, a clear trend was visible for ΔH_{tot}, showing significantly lower melting enthalpies, corresponding to lower equilibrium SFCs, with increasing concentrations of limonene (Table 5). This observation is consistent with the study of Do et al. (2008) who stated that limonene, which does not crystallize itself at 18°C, may act as a physical barrier preventing the crystallization of cocoa butter, and thus resulting in a marked decrease in crystallinity.

The crystal morphology and number of crystals formed during isothermal crystallization at 18°C of pure cocoa butter and cocoa butter samples with addition of 2.5% and 7.5% limonene were visualized by PLM at time intervals of 10 min (Figure 6). During the first 20 minutes fewer crystals were formed with addition of 2.5% limonene in comparison with the pure cocoa butter and very few with addition of 7.5% limonene. However, at 30 minutes larger structures could be detected in samples that contain limonene suggesting that the microstructure was very rapidly formed between 20 and 30 minutes and that with a lower amount of crystals a network was already formed. Especially for the case of 7.5% limonene, this development was noteworthy. The microstructure was still evolving until 40 minutes, resulting in a crystal network with larger structures for the samples containing limonene than in the case of the pure cocoa butter. In addition, a larger number of dark regions was visible for the samples with limonene, and in particular for 7.5%, indicating more liquid content. Again these observations are in agreement with Ray et al. (2011) who observed that after 1 day of storage at 20°C the samples containing 5% limonene exhibit much larger and distinct feather-shaped spherulites compared with the pure cocoa butter, which confirms that limonene leads to larger structures.

4.2.3 Comparison of ultrasonic and conventional techniques

The use of different analysis techniques allows us to compare and relate the parameters of the inverse model of the proposed ultrasonic shear reflection technique to the observations of the conventional techniques. First of all, we notice that the kinetic parameter t_{ind}, resulting from the swRC inversion (Table 4), does not match the trends of the DSC parameter, $t_{onset.}$ (Table 5). Furthermore, a clear downward trend was observed for the K parameter with the ultrasonic technique (Table 4), while no systematic trend was observed in the time difference of t_{onset} and t_{peak} (Table 5), suggesting that limonene had no clear impact on the crystal growth rate of the primary crystallization. In contrast, PLM demonstrated that the microstructure developed much faster with the addition of limonene, especially with the addition of 7.5% (Figure 6), which agrees with the observed trend of the parameter K deduced from the proposed ultrasonic

technique (Table 4). This implies that t_{ind} more readily indicates the start of the microstructure development instead of the crystal formation, and that K should be regarded as the rate of network formation.

The decreasing trend in v_{s2} with increasing limonene concentration (Table 4) does correlate with the decreasing ΔH_{tot} (Table 5), and thus with the SFC, even though only the v_{s2}-values for 5% and 7.5% limonene were significantly lower than v_{s2} of the reference sample of pure cocoa butter (Table 4). It cannot be ruled out however that also the aggregation of the crystals affected v_{s2}. The larger structures with addition of limonene showed less inter-particle links (Figure 6), which might also result in a decrease of v_{s2}, leading to a cumulative effect. The fact that the attenuation was similar for all samples (Table 4), seems to contradict the clear downward trend in ΔH_{tot} (Table 5), which is correlated with the SFC. However, PLM showed that the presence of limonene caused the formation of larger structures (Figure 6), which may also influence the attenuation of ultrasonic waves (Martini et al., 2005c), and both effects may cancel out each other. This suggests that a_{s2} in the ultrasonic shear reflection technique is not only determined by the SFC but also by the developed microstructure.

Conclusion

The ultrasonic shear reflection technique is only sensitive for a sample with a certain microstructure development as shear waves need an elastic material to be propagated. Therefore, the technique does not measure the primary crystallization, but monitors the microstructural development with the crystals aggregating to form a three-dimensional elastic network. This makes the ultrasonic shear reflection technique an interesting monitoring tool complementary to techniques that measure the primary crystallization such as DSC. Both information about the kinetic aspects of the microstructure development (t_{ind} and K) as the microstructure itself (v_{s2} and a_{s2}) can be obtained simultaneously by this non-destructive technique which also offers potential to be applied inline.

Acknowledgments

This work was funded by the Fund for Scientific Research-Flanders, Belgium (FWO) by a scholarship for Annelien Rigolle and the KU Leuven BOF STRT1/10/015 project. The authors would like to thank Barry Callebaut for the supply of cocoa butter.

References

Acevedo, N. C., Peyronel, F., & Marangoni, A. G. (2011). Nanoscale structure intercrystalline interactions in fat crystal networks. *Current Opinion in Colloid & Interface Science*, 16, 374–383.

Afoakwa, E., Paterson, A., Fowler, M., & Vieira, J. (2008). Modelling tempering behaviour of dark chocolates from varying particle size distribution and fat content using response surface methodology. *Innovative food science and emerging technologies*, 9, 527-533.Beckett, S.T. (2001). Preparation of chocolate with limonene to reduce fat content. US Patent 6,200,625.

Bolliger, S., Zeng, Y., & Windhab, E. J. (1999). In-line measurement of tempered cocoa butter and chocolate by means of near-infrared spectroscopy. *Journal of the American Oil Chemists' Society, 76(6),* 659-667.

Brunello, N., McGauley, S. E., & Marangoni, A. (2003). Mechanical properties of cocoa butter in relation to its crystallization behavior and microstructure. *LWT- Food Science and Technology, 36,* 525-532.

Chapman, G. M., Akehurst, E. E. & Wright, W.B. (1971). Cocoa butter and confectionery fats. Studies using programmed temperature X-ray diffraction and differential scanning calorimetry. *Journal of the American Oil Chemists' Society, 48,* 824-830.

De Graef, V., Dewettinck, K., Verbeken, D., & Foubert, I. (2006). Rheological behavior of crystallizing palm oil. *European Journal of Lipid Science and Technology, 108,* 864-870.

Dhonsi, D., & Stapley, A.G.F., The effect of shear rate, temperature, sugar and emulsifier on the tempering of cocoa butter. *Journal of Food Engineering, 77*, 936-942.

Do, T.-A.L., Vieira, J., Hargreaves, J.M., Wolf, B. and Mitchell, J.R. (2008). Impact of limonene on the physical properties of reduced fat chocolate. *Journal of the American Oil Chemists' Society, 85*, 911-920.

Foubert, I., Vanrolleghem, P. A., Vanhoutte, B., & Dewettinck, K. (2002). Dynamic mathematical model of the crystallization kinetics of fats. *Food Research International, 35,* 945-956.

Foubert, I., Dewettinck, K., & Vanrolleghem P. A. (2003). Modelling of the crystallization kinetics of fats. *Trends in Food Science & Technology, 14*, 79-92.

Garbolino, C., Ziegler, G. R., & Coupland, J. N. (2000). Ultrasonic determination of the effect of shear on lipid crystallization. *Journal of the American Oil Chemists' Society, 77*, 157-162.

Ghotra, B. S., Dyal, S. D., & Narine, S. S. (2002). Lipid shortenings: a review. *Food Research International, 35*, 1015-1048.

Häupler, M., Peyronel, F., Neeson, I., Weiss, J., & Marangoni, A. (2014). In situ ultrasonic characterization of cocoa butter using a chirp. *Food and Bioprocess Technology, 7(11),* 3186-3196.

Hishamuddin, E., Stapley, A. G. F., & Nagy, Z. K. (2011). Application of laser backscattering for monitoring of palm oil crystallization from melt. *Journal of Crystal Growth, 335,* 172-180.

Létang, C., Piau, M., Verdier, C., & Lefebvre, L. (2001). Characterization of wheat-flour-water doughs: a new method using ultrasound. *Ultrasonics, 39,* 133-141.

Maleky, F., & Marangoni, A. (2011). Ultrasonic technique for determination of the shear elastic modulus of polycrystalline soft materials. *Crystal growth & Design, 11,* 941-944.

Marangoni, A. G., Acevedo, N., Maleky, F., Co, E., Peyronel, F., Mazzanti, G., Quinn, B., & Pink, D. (2012). Structure and functionality of edible fats. *Soft Matter, 8,* 1275-1300.

Martini, S., Herrera, M. L., & Marangoni, A. (2005a). New technologies to determine solid fat content on-line. *Journal of the American Oil Chemists' Society, 82(5),* 313-317.

Martini, S., Bertoli, C., Herrera, M. L., Neeson, I., & Marangoni, A. (2005b). *In situ* monitoring of solid fat content by means of pulsed nuclear magnetic resonance spectrometry and ultrasonics. *Journal of the American Oil Chemists' Society, 82(5),* 305-312.

Martini, S., Bertoli, C., Herrera, M.L., Neeson, I., & Marangoni, A. (2005c). Attenuation of ultrasonic waves : influence of microstructure and solid fat content. *Journal of the American Oil Chemists' Society, 82,* 319-328.

McClements, D. J. (1997). Ultrasonic characterization of foods and drinks: principles, methods, and applications. *Critical Reviews in Food Science and Nutrition, 37(1),* 1-46.

Miyasaki, E. K., dos Santos, C. A., Vieira, L. R., Ming, C. C., Calligaris, G. A., Cardoso, L. P., Gonçalves, L. A. G. (2015). Acceleration of polymorphic transition of cocoa butter and cocoa butter equivalent by addition of D-limonene. *European Journal of Lipid Science and Technology,*

Narine, S.S., & Marangoni, A.G. (1999). Relating structure of fat crystal networks to mechanical properties: a review. *Food Research International, 32,* 227-248.

Patist, A., & Bates, D. (2008). Ultrasonic innovations in the food industry: From the laboratory to commercial production. *Innovative food science and emerging technologies,* 9, 147-154.

Talbot, G. (2009) Vegetable fats. In S.T. Beckett (Ed.), Industrial chocolate manufacture and use (pp. 415-433). Oxford: Blackwell Publishing Ltd.

Ray, J., MacNaughtan, W., Chong, P.S., Vieira, J. , & Wolf, B. (2011). The Effect of Limonene on the Crystallization of Cocoa Butter. *Journal of the American Oil Chemists' Society, 89,* 437-445.

Rigolle, A., Foubert, I., Hettler, J., Verboven, E., Demuynck, R., & Van Den Abeele, K. (2015). Development of an ultrasonic shear reflection technique to monitor the crystallization of cocoa butter. *Food Research International, 75,* 155-122.

Saggin, R., & Coupland, J. N. (2004). Shear and longitudinal ultrasonic measurements of solid fat dispersions. *Journal of the American Oil Chemists' Society, 81(1),* 27-32.

Singh, A. P., McClements, D. J., & Marangoni, A. G. (2004). Solid fat content determination by ultrasonic velocimetry. *Food Research International, 37,* 545-555.

Svenstrup, G., Heimdal, H., & Norgaard, L. (2005). Rapid instrumental methods and chemometrics for the determination of pre-crystallization in chocolate. *International Journal of Food Science and Technology, 40,* 953-962.

Wu, D., & Sun, D. (2013). Advanced applications of hyperspectral imaging technology for food quality and safety analysis and assessment: a review - Part II: Applications. *Innovative food science and emerging technologies*, 19, 15-28.

Table 2: Parameters of the ultrasonic shear reflection technique obtained by the inverse model: the induction time (t_{ind}), the growth rate (K), the shear ultrasonic velocity (v_{s2}) and the shear ultrasonic attenuation coefficient (a_{s2}) for pure cocoa butter isothermally crystallized at 18°C and 20°C.

$T_{isotherm}$ (°C)	t_{ind} (min)	K (1/min)	v_{s2} (m/s)	a_{s2} (-)
18°C	23.5 ± 5.4^{A}	0.0054 ± 0.0004^{A}	586 ± 46^{A}	0.165 ± 0.029^{A}
20°C	32.5 ± 3.0^{B}	0.0046 ± 0.0001^{B}	539 ± 12^{B}	0.141 ± 0.012^{A}

Mean values ± standard deviations. Values within one parameter with the same letter are not significantly different ($p<0.05$).

Table 3: DSC parameters of the isothermal crystallization curve of pure cocoa butter measured at 18°C and 20°C: peak onset (t_{onset} (min)) and peak maximum (t_{peak} (min)) of the crystallization curve and the total melting enthalpy (ΔH_{tot} (J/g)).

Temperature	***t_{onset} (min)***	***t_{peak} (min)***	***ΔH_{tot} (J/g)***
18 °C	19.8 ± 0.6^{A}	27.0 ± 0.5^{A}	103.5 ± 0.8^{A}
20 °C	25.3 ± 1.1^{B}	33.3 ± 1.4^{B}	96.5 ± 1.1^{B}

Mean values ± standard deviations. Values within one parameter with the same letter are not significantly different ($p<0.05$).

Table 4: Parameters of the ultrasonic shear reflection technique: the induction time (t_{ind}), the growth rate (K), the shear ultrasonic velocity (v_{s2}) and the shear ultrasonic attenuation coefficient (a_{s2}), resulting from the inverse model for pure cocoa butter and cocoa butter blends containing 1%; 2.5%; 5% and 7.5% limonene isothermally crystallized at 18°C.

Concentration limonene (%)	t_{ind} *(min)*	*K (1/min)*	v_{s2} *(m/s)*	a_{s2} *(-)*
0%	23.5 ± 5.4^{A}	0.0054 ± 0.0004^{A}	586 ± 46^{A}	0.165 ± 0.029^{A}
1%	25.3 ± 3.9^{A}	$0.0056 \pm 0.0001^{A,B}$	$549 \pm 31^{A,B}$	0.186 ± 0.035^{A}
2.5%	25.6 ± 2.7^{A}	$0.0061 \pm 0.0006^{A,B}$	$549 \pm 34^{A,B}$	0.162 ± 0.032^{A}
5%	26.7 ± 1.7^{A}	$0.0061 \pm 0.0005^{A,B}$	$485 \pm 14^{B,C}$	0.152 ± 0.038^{A}
7.5%	23.1 ± 2.0^{A}	0.0067 ± 0.0013^{B}	467 ± 28^{C}	0.164 ± 0.096^{A}

Mean values ± standard deviations. Values within one parameter with the same letter are not significantly different ($p<0.05$).

Table 5: DSC parameters for the isothermal crystallization of pure cocoa butter and cocoa butter blends containing 1%; 2.5%; 5% and 7.5% limonene at 18°C: peak onset (t_{onset} (min)) and peak maximum (t_{peak} (min)) of the crystallization curve and the total melting enthalpy (ΔH_{tot} (J/g)).

Concentration limonene (%)	t_{onset} *(min)*	t_{peak} *(min)*	ΔH_{tot} *(J/g)*
0%	19.8 ± 0.6^{A}	27.0 ± 0.5^{A}	103.5 ± 0.8^{A}
1%	16.7 ± 0.3^{B}	23.5 ± 0.4^{B}	97.0 ± 0.8^{B}
2.5%	15.8 ± 1.6^{B}	23.0 ± 1.1^{B}	90.6 ± 0.5^{C}
5%	17.7 ± 1.1^{B}	23.5 ± 1.0^{B}	78.4 ± 2.6^{D}
7.5%	22.7 ± 1.6^{C}	28.9 ± 1.5^{C}	68.9 ± 2.3^{E}

Mean values ± standard deviations. Values within one parameter with the same letter are not significantly different ($p<0.05$).

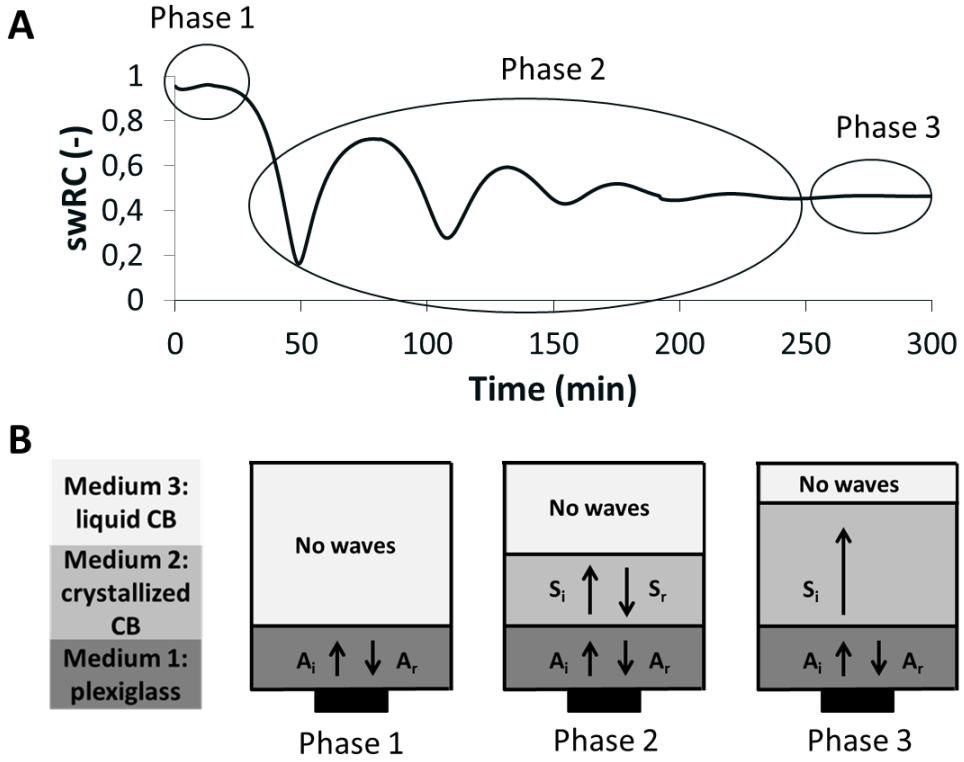

Figure 1: Principle of the ultrasonic shear reflection technique: schematic representation of the link between the typical pattern of the swRC (A) and the propagation of shear waves (B) at three distinct phases during the isothermal crystallization of cocoa butter.

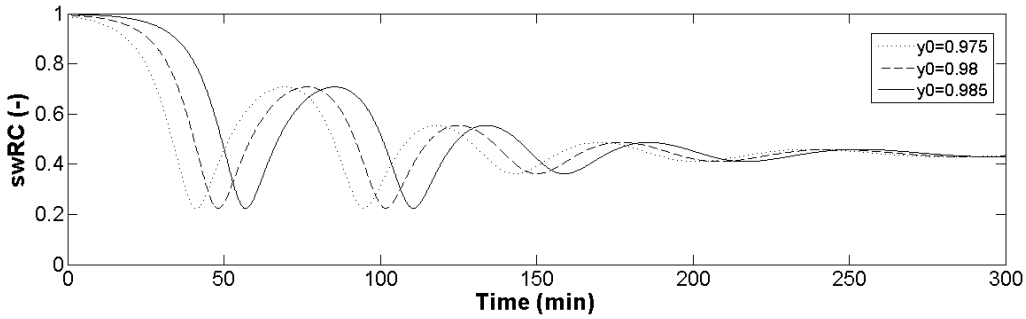

Figure 2: Illustration of the influence of the parameter y_0 on the swRC as function of the crystallization time (min). The parameter y_0 is varied between 0.975; 0.98 and 0.985. The other model parameters are fixed: n=8; K=0.005/min; d*=0.002m; v_{s2}=600m/s; a_{s2}=0.15. The shear wave frequency equals 1MHz.

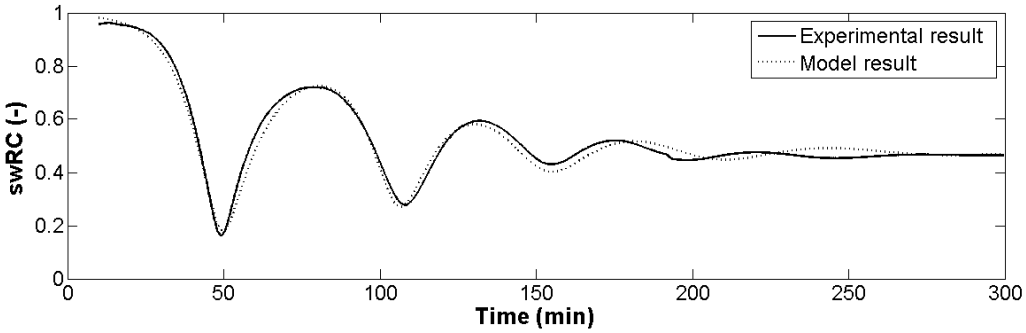

Figure 3: Overlay of an experimental and model result of the evolution of the swRC in function of time (min) during the isothermal crystallization of pure cocoa butter at 20°C with n and d* fixed to 8 and 0.002 m respectively.

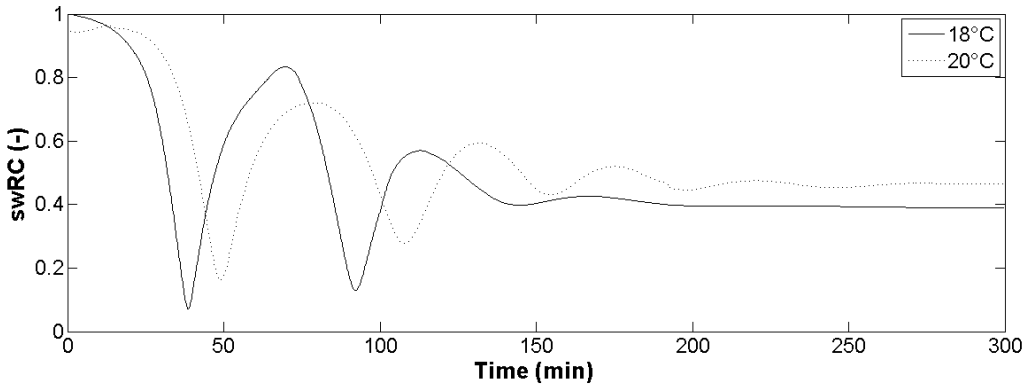

Figure 4: Overlay of the evolution of the swRC in time (min) during the isothermal crystallization of pure cocoa butter measured at 18°C and 20°C. One representative curve is displayed for both temperatures. The measurements were carried out on independent samples and a frequency of 1 MHz was used.

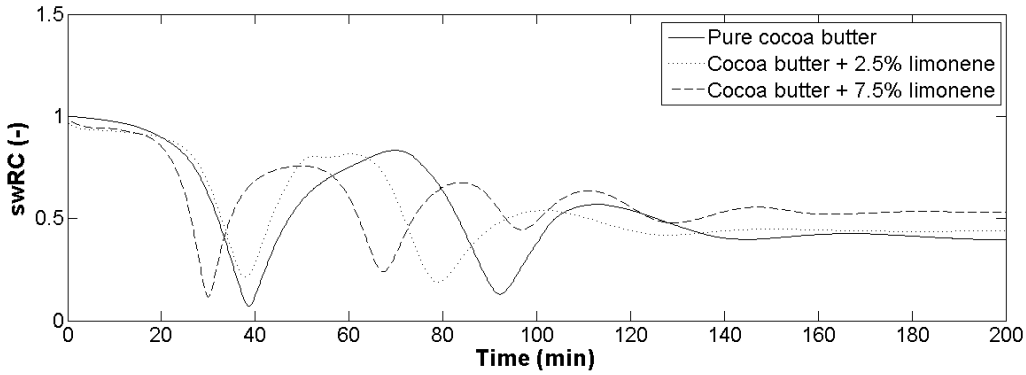

Figure 5: Overlay of the evolution of the swRC in time (min) during the isothermal crystallization at 18°C of pure cocoa butter and cocoa butter blends containing 2.5% and 7.5% limonene. One representative curve is displayed for each concentration and a frequency of 1 MHz was used.

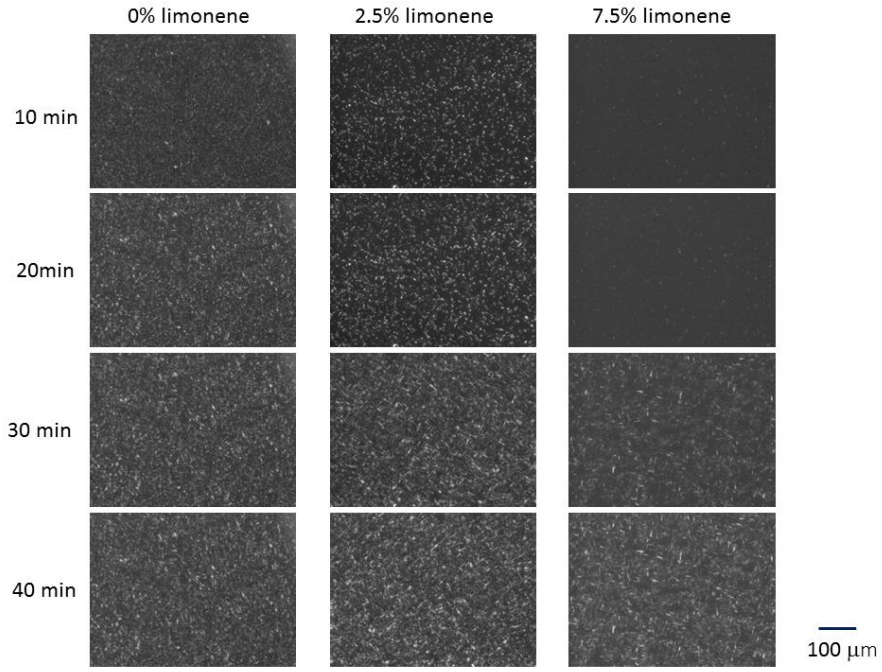

844

845 Figure 6: PLM images of cocoa butter added with 2.5 % (w/w) and 7.5 % (w/w) limonene after different
846 periods of isothermal crystallization at 18°C.

847

848

849

850

851

852

853